Bootstrap Tomography of the Pulses for Quantum Control

V. V. Dobrovitski,[1] G. de Lange,[2] D. Ristè,[2] and R. Hanson[2]

[1]*Ames Laboratory, U.S. DOE, Iowa State University, Ames Iowa 50011, USA*

[2]*Kavli Institute of Nanoscience Delft, Delft University of Technology, Post Office Box 5046, 2600 GA Delft, The Netherlands*

(Received 19 April 2010; revised manuscript received 16 July 2010; published 11 August 2010)

Long-time dynamical decoupling and quantum control of qubits require high-precision control pulses. Full characterization (quantum tomography) of imperfect pulses presents a bootstrap problem: tomography requires initial states of a qubit which cannot be prepared without perfect pulses. We present a protocol for pulse error analysis, specifically tailored for a wide range of the single solid-state electron spins. Using a single electron spin of a nitrogen-vacancy center in diamond, we experimentally verify the correctness of the protocol, and demonstrate its usefulness for quantum control tasks.

DOI: 10.1103/PhysRevLett.105.077601 PACS numbers: 76.30.Mi, 03.65.Wj, 76.60.−k

Coherent manipulation of single and a few electron spins has recently been achieved in several solid-state systems such as quantum dots and diamond defect centers. Such systems are promising candidates for quantum information processing [1,2], precise metrology [3], and ultrasensitive magnetometry [4]. They also present an excellent testbed for studying the fundamental problems of quantum dynamics of open systems [5–7]. High-speed manipulation of the system's quantum state can be achieved by using microwave or optical pulses [8–10], which must be fine-tuned to provide a high degree of fidelity. For example, sequences of quantum control pulses can be used to extend the coherence time via dynamical decoupling [11–15]. For long sequences, even small errors in the pulses will destroy the coherence that one attempts to preserve [14,16] and may even lead to artificial saturation [17,18]. Therefore, precise characterization of errors is essential for successful implementation of complex quantum control protocols. With known errors, composite pulses and/or special pulse sequences can be chosen to mitigate the problem.

Complete information on the action of a pulse can in principle be gained with quantum process tomography (QPT) [19]. However, QPT of an imperfect pulse requires preparation and measurement of a complete set of reference states, whereas in many solid-state qubit systems (e.g., quantum dots, diamond defect centers, superconducting circuits) only one state can be prepared reliably (without the imperfect pulses), and only one observable can be directly measured. All other states can be prepared only with the imperfect pulses themselves, and therefore have errors [20]. This presents a bootstrap problem: the reference states contain the very same errors that we want to determine.

The problem of pulse error analysis has been studied extensively in the areas of NMR and ESR [21–24]. However, single electron spins in solid-state settings present new opportunities and challenges, and call for new approaches tailored at the specific demands of these systems. The driving pulse field can be tightly confined in the vicinity of the target spin. The resulting strong, nanosecond time scale pulses enable fast spin manipulation, but the standard pulse error analysis [21–25] used in NMR becomes inapplicable. At strong driving, the spin dynamics changes noticeably [10]. The nonsecular terms in the rotating frame can become important. The ac-Stark and Bloch-Siegert shifts can significantly detune the pulse frequency from resonance [10] and tilt the rotation axis towards the z axis. Also, the pulse edges constitute a much larger fraction of the short pulse, and the driving field at the edges varies much faster and stronger than in typical NMR pulses. The resulting errors [10] (e.g., tilting of the rotation axis) can go beyond the standard treatment [26], and cannot always be removed by symmetrizing the pulse shape.

Also, typical NMR systems have long coherence times that exceed the pulse width by orders of magnitude. The standard tune-up protocols [21–24] exploit this advantage, and use sequences with tens or hundreds of pulses to achieve outstanding precision in pulse parameters. But single solid-state electron spins are dephased faster, on a time scale T_2^* of microseconds down to tens of nanoseconds [5]. After only tens of pulses the signal becomes a complex mixture of pulse errors and decoherence [17,18]. To ensure a reliable measurement of the errors, the sequences for single electron spins must be short so that decoherence during each sequence would be negligible.

Here, we present a systematic approach to pulse characterization for single solid-state electron spins, which is usable at shorter coherence times and much stronger driving power compared to traditional NMR systems. The proposed protocol contains four series of measurements, each having only 1–3 pulses, thus minimizing the effect of decoherence. The measured signal quantifying the pulse errors grows linearly with the errors to ensure a good accuracy for small errors. Also, the signal is zero for zero errors for good relative accuracy. The protocol determines all pulse errors: the rotation angle and all three components of the rotation axis [26]. We experimentally demonstrate the protocol on a single spin of a nitrogen-vacancy (NV)

defect center in diamond. By deliberately introducing known pulse errors, we verify the accuracy and self-consistency of the protocol, and use it to significantly increase the fidelity of QPT.

Our goal is to determine the parameters of four pulses, π_X, π_Y, $\pi/2_X$, and $\pi/2_Y$ applied to a two-level quantum system (π_X denotes a rotation by an angle π around the x axis in the rotating frame; the other notation is analogous). Minimization of the pulse errors and pulse optimization are not the subjects of this Letter. This set of pulses allows implementation of universal decoupling XY sequences [11,12], full tomography of the density matrix, and universal single-qubit gates [19]. We assume that the pulse errors are reasonably small, and consider only the first-order terms in these quantities (since we want the signal to grow proportionally to errors). We also assume that the pulse width t_p is small in comparison with the dephasing time T_2^*; in this case the impact of decoherence is of second order, $(t_p/T_2^*)^2$, and is negligible for short sequences [26]. Under this assumption the evolution of a spin during the pulse can be described as a unitary rotation. For example, for $S = 1/2$, the evolution (in the rotating frame) during an imperfect π_X pulse is given by

$$U_X = e^{-i(\vec{n}\,\vec{\sigma})(\pi+2\phi)/2} \approx -\phi\mathbf{1} - i(\sigma_x + \epsilon_y\sigma_y + \epsilon_z\sigma_z), \tag{1}$$

where $\sigma_{x,y,z}$ are the Pauli matrices, 1 is a 2×2 identity matrix, the rotation angle error is 2ϕ, and the rotation axis $\vec{n}$ has small components $n_y = \epsilon_y$ and $n_z = \epsilon_z$. Similarly, a $\pi/2_X$ pulse U_X' has the rotation angle error $2\phi'$, and the small rotation axis components ϵ_y' and ϵ_z' along y and z, respectively. Note that two $\pi/2$ pulses do not yield the same evolution as one π pulse due to errors introduced by the pulse edges. Analogous parameters for y pulses will be denoted as 2χ, υ_x, and υ_z (angle and axis errors for π_Y), and $2\chi'$, υ_x', and υ_z' (angle and axis errors for $\pi/2_Y$).

The bootstrap protocol shares ideas with standard QPT, and with the NMR tune-up sequences. Before each measurement, the spin is in the state $|\uparrow\rangle$, and the measured signal is $\langle\psi|\sigma_z|\psi\rangle$, where $|\psi\rangle$ is the wave function after the pulse. The preparation and the readout axes are usually fixed: e.g., for NV centers, they both coincide with one of the crystallographic $\langle 111\rangle$ directions. A possible mismatch between these axes in other systems can be taken into account, but complicates the protocol, and is not considered here. An imperfect pulse U_j can be represented as a product $U_j = U_j^{(0)}V_j \approx U_j^{(0)}(1 - iK_j)$, where $U_j^{(0)}$ is a corresponding ideal rotation and the Hermitian operator K_j is proportional to small pulse errors. Applying two pulses U_1 and U_2 in succession, we obtain up to linear order in K_j

$$U_{21} = U_2U_1 \approx U_2^{(0)}U_1^{(0)} - iU_2^{(0)}K_1 - iK_2U_1^{(0)}, \tag{2}$$

and the terms $U_2^{(0)}K_1$ and $K_2U_1^{(0)}$ contain different matrix elements of the operators K_1 and K_2. E.g., if U_1 and U_2 are the (imperfect) $\pi/2_Y$ and $\pi/2_X$ rotations, the signal detected after this sequence, $S_{21} = \mathrm{Tr}(\sigma_z U_{21}|\uparrow\rangle\langle\uparrow|U_{21}^\dagger)$, contains a linear combination of the matrix elements $\langle\uparrow|K_1|Y\rangle$ and $\langle\uparrow|K_2|X\rangle$ (where $|Y\rangle = |\uparrow\rangle + i|\downarrow\rangle$ and $|X\rangle = |\uparrow\rangle + |\downarrow\rangle$). Combining different pulses, we obtain a sufficient number of such linear combinations of various matrix elements of K_j to uniquely determine all of them. A general approach to bootstrap tomography can be formulated in the language of QPT, by expanding the operation element operators [19] in terms of small errors. More complex bootstrap protocols applicable to more complex systems (higher spins, few qubits, etc.) can be designed in a similar manner. Here, we focus on a single two-level system.

The protocol is summarized in Table I. It consists of three blocks of measurement sequences. For each sequence the measured signal is given in terms of the error parameters. The first block, with two single-pulse sequences, yields the rotation angle errors for the $\pi/2$ pulses. This information is then used in the second block, consisting of four two-pulse sequences, to find the rotation angle errors and the components of the rotation axis along z for the π pulses. The third block has six multipulse sequences, yielding six signals that are linearly related to the remaining six pulse error parameters. This linear system is underdetermined, since the whole system of pulses is invariant under rotations around the z axis. We may put $\epsilon_y' = 0$, taking the phase of the $\pi/2_X$ pulse as the x direction in the rotating frame. This fixes all other directions, and all errors are uniquely determined. No unphysical results appear in this bootstrap protocol: in experiments below, we use the bare measurement data imposing no additional conditions.

We now demonstrate and verify the protocol experimentally by applying it to a single solid-state spin system. We use the spin of a single NV center, which is a defect in diamond composed of a substitutional nitrogen atom with an adjacent vacancy [27]. The NV center's spin can be optically polarized and readout [27]. The unpolarized part of the spin's density matrix is proportional to the identity

TABLE I. Summary of the bootstrap protocol: pulse sequences (read from right to left) and the resulting signals expressed in terms of the error parameters.

Sequence	Signal
$\pi/2_X$	$-2\phi'$
$\pi/2_Y$	$-2\chi'$
$\pi/2_X - \pi_X$	$2(\phi + \phi')$
$\pi/2_Y - \pi_Y$	$2(\chi + \chi')$
$\pi_Y - \pi/2_X$	$-2\upsilon_z + 2\phi'$
$\pi_X - \pi/2_Y$	$2\epsilon_z + 2\chi'$
$\pi/2_Y - \pi/2_X$	$-\epsilon_y' - \epsilon_z' - \upsilon_x' - \upsilon_z'$
$\pi/2_X - \pi/2_Y$	$-\epsilon_y' + \epsilon_z' - \upsilon_x' + \upsilon_z'$
$\pi/2_X - \pi_X - \pi/2_Y$	$-\epsilon_y' + \epsilon_z' + \upsilon_x' - \upsilon_z' + 2\epsilon_y$
$\pi/2_Y - \pi_X - \pi/2_X$	$-\epsilon_y' - \epsilon_z' + \upsilon_x' + \upsilon_z' + 2\epsilon_y$
$\pi/2_X - \pi_Y - \pi/2_Y$	$\epsilon_y' - \epsilon_z' - \upsilon_x' + \upsilon_z' + 2\upsilon_x$
$\pi/2_Y - \pi_Y - \pi/2_X$	$\epsilon_y' + \epsilon_z' - \upsilon_x' - \upsilon_z' + 2\upsilon_x$

matrix, and gives no contribution to the signal (i.e., the NV spin state is pseudopure as in traditional NMR/ESR). The experiments are performed in a home-built confocal microscope at room temperature. NV centers in nanocrystals are prepared on a chip with a lithographically defined waveguide allowing fast and precise spin rotations by magnetic resonance [26].

We controllably introduce two types of pulse errors, and use the bootstrap protocol to extract their values. First, we vary the phase Φ of the nominal $\pi/2_Y$-pulse between $-30°$ and $30°$ from its nominal value. In this way, we are changing the error parameter $v_x' = -\sin\Phi \approx -\Phi(\mathrm{rad})$, while leaving all other errors constant. Figure 1(a) shows the experimental results that clearly support this expectation.

In the second experiment we detune the microwave excitation away from the qubit transition frequency, thereby varying the z components of the rotation axis for all pulses. As shown in Fig. 1(b), the extracted error parameters v_z, v_z', ϵ_z, and ϵ_z' strongly change (roughly linearly) with the detuning as expected, while the other error parameters stay virtually constant. The errors of the nominal $\pi/2$ pulses vary about twice as much as the errors of the nominal π pulses, indicating that the errors originate largely from the pulse edges. Since the edges are the same for all pulses, they have larger impact on shorter pulses. The data in Figs. 1(a) and 1(b) demonstrate that the bootstrap protocol is indeed an effective and reliable tool for extracting pulse errors.

Because of experimental limitations it may be impossible to cancel all errors at once. In that case, the choice of the optimal working point involves a trade off, and precise knowledge of the pulse errors becomes particularly important. For example, when performing QPT, a set of the reference states is prepared using the pulses π_X, $\pi/2_X$, and $\pi/2_Y$. These states are acted upon by the process, and rotated to the readout basis before measurement [19]. The operation elements of the quantum process are expanded in the basis $E_0 = I, E_1 = \sigma_x, E_2 = \sigma_y$, and $E_3 = \sigma_z$, and the process is completely characterized by the 4×4 expansion matrix χ [19]. When systematic pulse errors are present, the prepared initial states differ from the reference states, and the readout is also performed in the incorrect basis, yielding an incorrect matrix χ. But with pulse errors known, the raw measured data can be transformed into the correct basis prior to the standard QPT data processing [19,20,28].

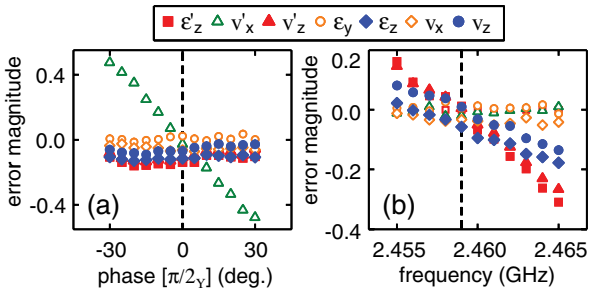

FIG. 1 (color online). Experimental verification of the bootstrap protocol by introducing varying pulse errors. Duration of the $\pi/2$ pulses (π pulses) is 5 ns (9 ns). (a) Measured error parameters for different phases Φ of the $\pi/2_Y$ pulse. The frequency of the driving field is set at 2.4605 GHz. (b) Measured error parameters for various frequencies of the driving field. Error bars everywhere are smaller than the symbol size.

As a demonstration, and as a check of self-consistency of the bootstrap protocol, we perform QPT while introducing the same pulse errors as in Fig. 1. We show that with the pulse errors deduced with the protocol, the QPT results can be corrected. The comparison between raw and corrected data below is designed to use no *a priori* assumptions about correctness of the bootstrap protocol.

First, we take the (imperfect) π_Y pulse as an example of a quantum process. We introduce errors in the QPT procedure by changing the phase Φ of the nominal $\pi/2_Y$-pulse from $-30°$ to $30°$. We first determine the reference matrix of our quantum process. We perform QPT on this process using the $\pi/2_Y$ pulse with $\Phi = 0$, and the resulting reference matrix χ_0 is calculated in two ways: (i) using the raw uncorrected data, i.e., assuming that the pulses used for QPT are ideal (we denote this matrix as χ_0^r), and (ii) using the data corrected for the known pulse imperfections (the resulting matrix is χ_0^c). Next, we vary Φ, and use the artificially deteriorated $\pi/2_Y$ pulses to determine the matrix χ of the quantum process. This matrix is also determined in two ways, by using raw experimental data (matrix χ^r), and by correcting the data for the known pulse errors (matrix χ^c). For each value of Φ, we compare the raw-data

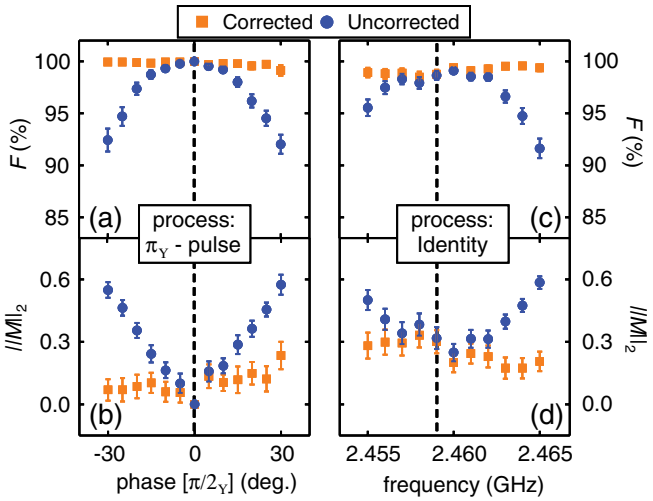

FIG. 2 (color online). Correction of pulse errors in Quantum Process Tomography using the bootstrap protocol. (a) Fidelity F and (b) the 2-norm distance $\|M\|_2$ between the process measured at finite introduced $\pi/2_Y$ phase error and the process matrix measured at zero introduced error. The process is a π_Y pulse with zero introduced error. Driving field frequency is 2.459 GHz. (c) F and (d) $\|M\|_2$ between the measured process and the actual process (identity). All measures are calculated both for the uncorrected and for the corrected data.

matrices χ^r and χ_0^r on one hand, and the corrected matrices χ^c and χ_0^c on the other.

The process we are studying does not depend on the phase of the nominal $\pi/2_Y$ pulse. Thus, ideally, the matrices χ_0 and χ should be the same. To quantify the difference between χ_0 and χ, we use two distance measures. One is the process fidelity [19] $F = \mathrm{Tr}[\chi_0\chi]$, which depends quadratically on the pulse errors. The other measure is the Hilbert-Schmidt 2-norm $\|M\|_2 = \sqrt{\mathrm{Tr}[MM^\dagger]}$ of the difference matrix $M = \chi - \chi_0$. This norm is linear in, and thus more sensitive to, the pulse errors.

In Figs. 2(a) and 2(b), orange squares show the values of F and $\|M\|_2$ for the corrected-data matrices χ_0^c and χ^c. The expectation that χ_0 and χ should coincide is confirmed with excellent precision. Almost independently of Φ, the fidelity remains above 99%, and $\|M\|_2$ stays small. This is not so for the raw-data matrices χ_0^r and χ^r (blue squares). The neglected phase error of the nominal $\pi/2_Y$ pulse makes the matrix χ^r inaccurate, so F and $\|M\|_2$ depend on Φ, with fidelity dropping by 8% for $\Phi = 30°$.

In a second experiment [Figs. 2(c) and 2(d)], we perform tomography on an identity process. The reference matrix χ_0 for an ideal identity process is known, and needs no measurement. We detune the microwave excitation frequency away from the qubit transition, introducing the errors ϵ_z, ϵ_z', υ_z, and υ_z' [like in Fig. 1(b)] into all pulses. We perform QPT on the identity process and, as above, determine the corrected and the uncorrected matrices χ^r, and χ^c. These matrices are compared with the *ideal* identity process. The results are shown in Figs. 2(c) and 2(d). Again, the fidelities are high for the corrected data in the full range of introduced errors, while for the uncorrected data the fidelity has dropped by as much as 10%. The same behavior is seen for $\|M\|_2$. The key point here is that the corrected matrix χ^c does not depend on the errors: orange points in Figs. 2(c) and 2(d) form a flat curve. Without correction (blue points), the measured χ matrix strongly depends on the pulse errors. Thus, even the effects of complex pulse errors introduced by detuning the frequency can be effectively corrected using the information from the bootstrap protocol.

Summarizing, we have developed and experimentally demonstrated an effective pulse error analysis protocol tailored to the specific requirements of single solid-state spins. The methods described in this paper may help in accurate determination of the properties of different quantum processes, a key feature for the fields of quantum information processing, quantum metrology and fundamental studies of quantum decoherence.

We would like to thank D. G. Cory, S. Lyon, A. Tyryshkin, M. Pruski, C. Ramanathan, K. Schmidt-Rohr, and M. Laforest for very useful and enlightening discussions. Work at Ames Laboratory was supported by the Department of Energy—Basic Energy Sciences under Contract No. DE-AC02-07CH11358. We gratefully acknowledge support from FOM, NWO, and the DARPA QuEST program.

[1] D. Loss and D. P. DiVincenzo, Phys. Rev. A **57**, 120 (1998).
[2] L. Childress *et al.*, Phys. Rev. Lett. **96**, 070504 (2006).
[3] J. A. Jones *et al.*, Science **324**, 1166 (2009); P. Cappellaro *et al.*, Phys. Rev. Lett. **94**, 020502 (2005); J. M. Geremia, J. K. Stockton and H. Mabuchi, Phys. Rev. Lett. **94**, 203002 (2005).
[4] J. M. Taylor *et al.*, Nature Phys. **4**, 810 (2008); C. Degen, Appl. Phys. Lett. **92**, 243111 (2008); G. Balasubramanian *et al.*, Nature (London) **455**, 648 (2008).
[5] R. Hanson and D. D. Awschalom, Nature (London) **453**, 1043 (2008).
[6] L. Childress *et al.*, Science **314**, 281 (2006); R. Hanson *et al.*, Science **320**, 352 (2008); D. J. Reilly *et al.*, Phys. Rev. Lett. **101**, 236803 (2008); C. Latta *et al.*, Nature Phys. **5**, 758 (2009); I. T. Vink *et al.*, Nature Phys. **5**, 764 (2009).
[7] C. H. Tseng *et al.*, Phys. Rev. A **61**, 012302 (1999); S. Lloyd, Science **273**, 1073 (1996).
[8] J. Berezovsky *et al.*, Science **320**, 349 (2008); D. Press *et al.*, Nature (London) **456**, 218 (2008); Y. Wu *et al.*, Phys. Rev. Lett. **99**, 097402 (2007).
[9] P. Neumann *et al.*, Science **320**, 1326 (2008); L. Jiang *et al.*, Science **326**, 267 (2009).
[10] G. D. Fuchs *et al.*, Science **326**, 1520 (2009).
[11] L. Viola, E. Knill, and S. Lloyd, Phys. Rev. Lett. **82**, 2417 (1999); L. F. Santos and L. Viola, Phys. Rev. Lett. **97**, 150501 (2006).
[12] K. Khodjasteh and D. A. Lidar, Phys. Rev. Lett. **95**, 180501 (2005).
[13] M. J. Biercuk *et al.*, Nature (London) **458**, 996 (2009).
[14] J. Du *et al.*, Nature (London) **461**, 1265 (2009).
[15] J. J. L. Morton *et al.*, Nature Phys. **2**, 40 (2006).
[16] H. De Raedt *et al.*, Prog. Theor. Phys. Suppl. **145**, 233 (2002).
[17] W. Zhang *et al.*, Phys. Rev. B **77**, 125336 (2008); W. Zhang *et al.*, J. Phys. Condens. Matter **19**, 083202 (2007).
[18] D. Li *et al.*, Phys. Rev. Lett. **98**, 190401 (2007).
[19] M. A. Nielsen and I. L. Chuang, *Quantum Computations and Quantum Information* (Cambridge University Press, Cambridge, England, 2002).
[20] J. M. Chow *et al.*, Phys. Rev. Lett. **102**, 090502 (2009).
[21] B. C. Gerstein and C. R. Dybowski, *Transient Techniques in NMR of Solids* (Academic, Orlando, 1985).
[22] D. P. Burum *et al.*, J. Magn. Reson. **43**, 463 (1981).
[23] A. J. Shaka *et al.*, J. Magn. Reson. **80**, 96 (1988).
[24] U. Haubenreisser and B. Schnabel, J. Magn. Reson. **35**, 175 (1979).
[25] J. J. L. Morton *et al.*, Phys. Rev. A **71**, 012332 (2005).
[26] See supplementary material at http://link.aps.org/supplemental/10.1103/PhysRevLett.105.077601.
[27] F. Jelezko and J. Wrachtrup, J. Phys. Condens. Matter **16**, R1089 (2004).
[28] M. Howard *et al.*, New J. Phys. **8**, 33 (2006).